Proceedings of the Korean Nuclear Society Autumn Meeting
Yongpyong, Korea, 2003

Cyclic deformation and damage mechanisms of 316L stainless steel and 308L weldment under low cycle fatigue and creep-fatigue at elevated temperature

F. Liu, J.G. Jung, S.W. Nam

Department of Materials Science and Engineering,
Korea Advanced Institute of Science and Technology,
373-1, Guseong-dong, Yuseong-gu, Daejeon, Korea 305-701

Abstract

Continuous low cycle fatigue (LCF) and creep-fatigue (CF) tests were conducted for both 316L base metal and 308L weldment at 550^{o}C and 600^{o}C. The cyclic stress response and Coffin-Manson plots were analyzed. Characterization of deformation microstructures and precipitated carbides after test was carried out by transmission electron microscopy (TEM) for the specimens of selected testing conditions. The initial cyclic hardening for 316L base metal is attributed to the increasing of dislocation density and the formation of dislocation cell and wall structure. The softening of base metal is resulted from the rearrangement of dislocations. Fully developed subgrains and the transformation from δ-ferrite to carbide might be the reason for the occurrence of saturation stage during creep-fatigue in weldment. Lower the carbon content may increase the creep-fatigue resistance of base metal. The weaker carbide/austenite interface formed during creep-fatigue test caused the reduction of creep-fatigue life in weldment.
Keywords: Creep; Fatigue life; dislocation; precipitation

1. Introduction

Because of their good corrosion and creep rupture resistance, the austenitic stainless steels are currently widely used in nuclear reactors and power plants. Numerous power plants, chemical plants and oil refineries are operated at high temperature or, more precisely, at temperature close to the creep regime of austenitic stainless steels. Statistics concerning boiler failures [1] reveal that creep, corrosion and low cycle fatigue of a component is usually of paramount importance. Therefore, specific attentions have been given to their resistance to low cycle fatigue (LCF) and creep. During the last decade, the numerous studies which have been made on the creep and cyclic behavior of these metals have considerably improved our understanding of the dislocation structures in relation to the cyclic strain-stress behavior and the crack initiation processes [2-6]. Among them, high temperature low cycle fatigue test with various tensile and compressive hold time are used to simulate the real conditions where the creep-fatigue interaction takes place. In comparison with continuous low cycle fatigue, fatigue tests with hold time at high temperature generally lead to a much reduced fatigue life [7, 8]. For austenite stainless

steels, tensile hold time during low cycle fatigue test was found to be more devastating, and the life reduction is a result of the occurrence of grain boundary cavitations [9, 10]. Since the nucleation of cavitations is tied up with grain boundary carbide, lowering the carbon content generally enhances the creep-fatigue resistance of austenite stainless steels. However, the deformation behavior and damage mechanism of welded joints that are subjected to creep–fatigue loading are not reported as frequently as those of base metal. Due to long-term exposure to creep–fatigue loading, weldment is subjected to degradation of mechanical properties, which is faster than that of the base metal [11, 12]. This is mainly due to the transformation from δ-ferrite to $M_{23}C_6$ carbides and some other brittle phases when it is exposed to elevated temperature. The degradation, together with stress-strain concentration that may occur within a joint can reduce the creep–fatigue life of welded joints, and in turn limit the life of the constructions..

In the present work, continuous low cycle fatigue and creep-fatigue tests at elevated temperature were conducted for both 316L base metal and 308L weldment. The cyclic deformation and fracture behavior were investigated. The precipitations inside δ-ferrite were carefully analyzed, and the relationship between the reduction of fatigue life with these precipitations was discussed.

2. Experimental procedure

Material

Commercial austenitic stainless steel 316L base metal and 308L weldment were used in the present investigation. Their chemical compositions are shown in Table 1. The 316L austenitic stainless steel was received as a hot-rolled plate with a thickness of 25mm. In order to reduce the residual stress induced by the hot-rolling, the material was aged at 1050^{o}C for one hour and cooled in air. In the center of the plates there was a thin band where there is much less δ-ferrite, this is originated from the continuous casting. However, the existence of this band has no influence on the tensile and fatigue results.

Table1. Chemical composition of base and weldment (wt%)

Alloy	C	Cr	Ni	Mo	Mn	N	S	P	Si	Fe
316L	0.025	16.83	10.24	2.03	1.19	0.03	0.002	0.019	0.56	Bal.
308L	0.03	18.8	9.5	0.055	1.18	0.06	0.023	0.037	0.76	Bal

Welding procedure

The gas tungsten arc welding process with the welding direction perpendicular to the rolling direction of the base metal was used to make weld deposits using 308L stainless steel welding rods of 2.6mm diameter. Welding was carried out using a current of 80-140A and a voltage of 10-16V with a torch travel speed of 8-15 cm/min. Typically, filling of this joint required 36 weld passes. All-weld specimens were taken from the weld pads prepared with a 20° included angle V-groove joint geometry. Weldment specimens were prepared perpendicular to the direction of welding travel. In order to make sure that weldment will be exactly located within the gauge length, special care was taken during specimen preparation.

Mechanical testing

Tensile tests were performed in an Instron 4206 testing machine with a strain rate of 0.004/s until final fracture. The test temperature was selected to be 500, 550, 600^{o}C. The specimens had a gauge diameter of 6mm and a gauge length of 25 mm. Prior to testing, the gauge section of specimens were ground with P2000 emery paper. Low cycle fatigue tests were performed in total strain control in a computer controlled Instron 1350 servo-hydraulic testing machine equipped with a reverberatory furnace which was heated by halogen photo optic lamps. The temperature was controlled by the thermal couple spot welded at the shoulder of the specimen. Before test, the thermal couple was calibrated by another thermal couple which was welded at the center of specimen. The fatigue specimens had a gauge length of 10 mm and a gauge diameter of 7mm. Before test, the specimens were ground with P2000 emery paper. In the fatigue test, a triangle waveform with zero mean strain (R=-1) was adopted with a mean strain rate of 0.004/s. The tests were carried out at total strain amplitudes of 0.4%, 0.5% and 0.6%. The test temperature was selected to be 550 and 600^{o}C. For creep-fatigue test, a 10 minutes tensile hold time was used. The critical number of cycles to failure, N_{cr}, was defined as the cycle number when the tensile peak stress had dropped to a value approximately 20% below the saturation stress on the cyclic hardening/softening curve. The tensile and compressive peak stresses were recorded during the test.

Electron microscopy

The surfaces of fractured specimens were investigated with a JSM 840A scanning electron microscope operated at 20 kV. The dislocation structures developed at different strain amplitudes, temperatures and at different testing waves were studied with JEOL 3000-EX microscope operated at 20KV. The TEM discs were cut from within the gauge section of the tested specimens. After carefully grinding down to about 50μm thickness and punched into small discs with a diameter of 3mm, thinning to perforation was performed electrolytically in 5 vol% perchloric acid + 95vol% acetic acid at 30V and 12.5^{o}C. Care was taken not to introduce additional dislocations during the sample preparation procedure. To certify this, comparisons were made in the TEM between fatigued material and undeformed material, prepared by the same procedure. Very low dislocation density was observed in the undeformed material, and it was therefore concluded that the TEM specimen preparation procedure did not introduce dislocations that could affect the results of the present study.

3. Results

3.1. Tensile deformation

Results from tensile tests for all the conditions are shown in Fig.1. We can clearly see that the elongation is much shorter for the weldment than for that of base metal, it indicates that the ductility is much lower for the weldment. Even though the yield strength is higher for weldment, the tensile strength is almost same with base metal. It is note worthy that there are zigzagged periods in all of the tensile test curves, and with increasing the temperature this phenomenon is more obvious. Some researcher suggested that this is due to the dynamic strain ageing, which is the interaction of solution atoms

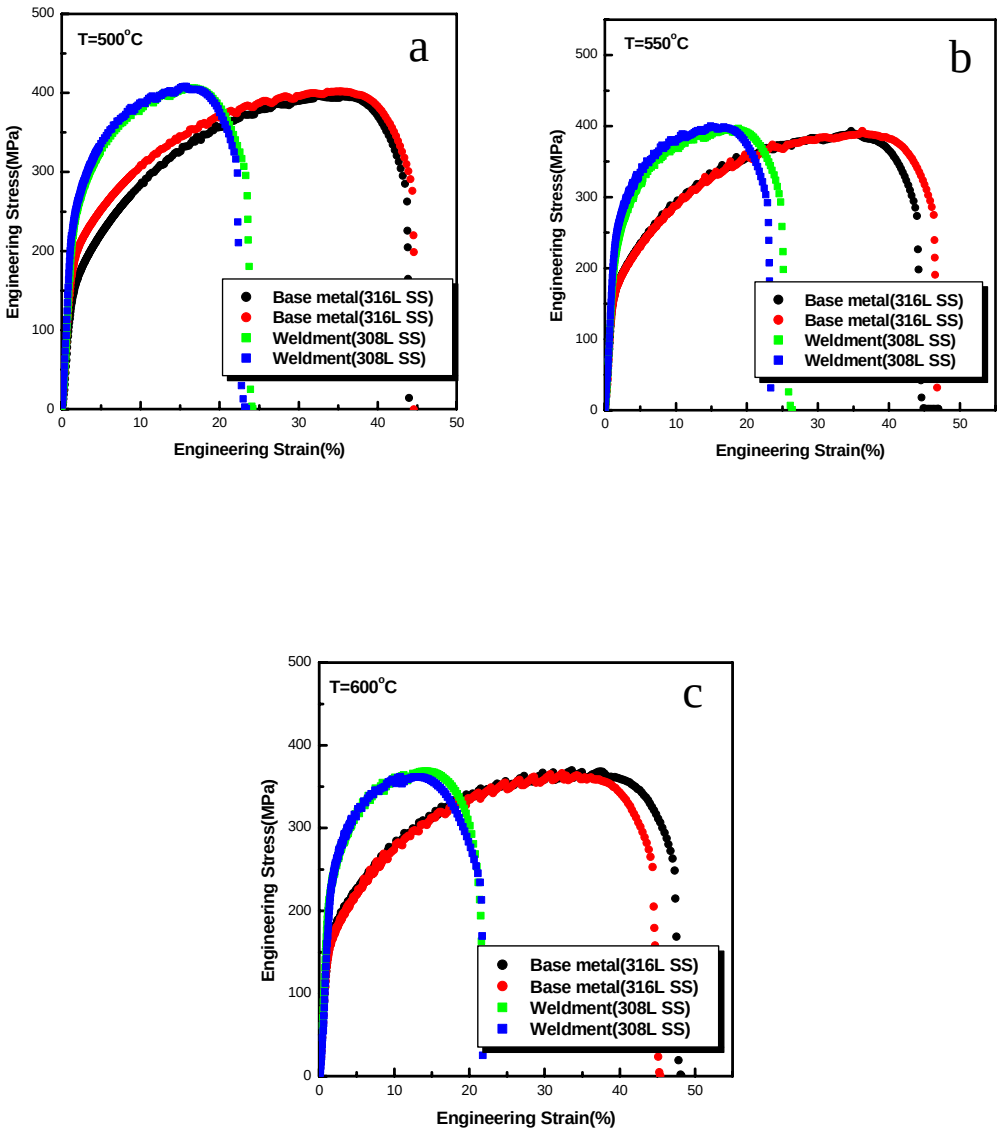

Fig. 1. Tensile test results for base metal, weldment and HAZ at
a) 500°C; b) 550°C; c) 600°C

with the moving dislocations [13]. However, it still couldn't successfully explain the prominent variation of flow stress during monotonic deformation.

3.2. Cyclic deformation

Cyclic hardening/softening.

Typical hardening/softening curves at the different testing conditions for both 316L base metal and 308L weldment are shown in Fig. 2. For the base metal, the curves have similar shapes during both continuous low cycle fatigue and creep-fatigue test, and initialhardening was observed at all test conditions. After tens (high strain amplitude) to

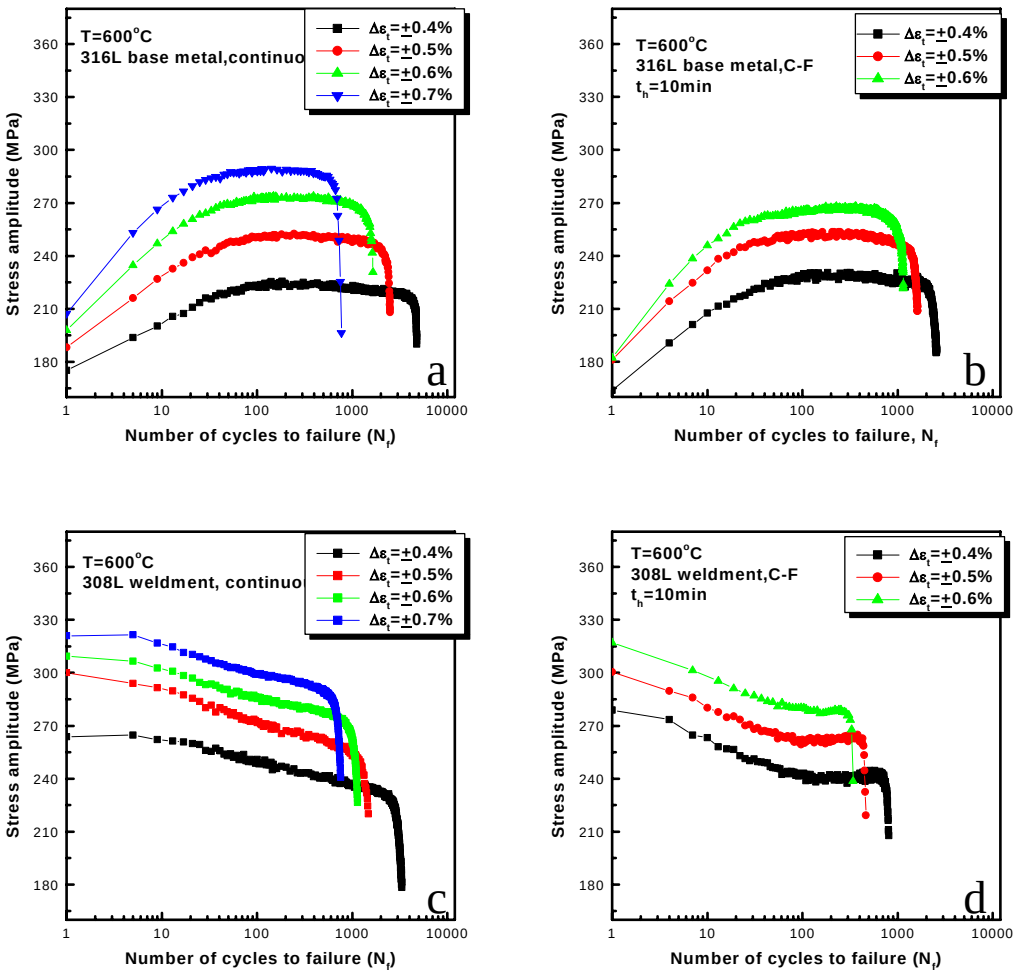

Fig. 2. Hardening/Softening curve for base metal a) continuous low cycle fatigue; b) creep-fatigue and weldment c) continuous low cycle fatigue; d) creep-fatigue

hundreds (low strain amplitude) of cycles, a saturation stage is occurred, which extends through the main part of the fatigue life (Fig.2 a, b). There is no subsequent hardening or softening until the final failure. In contrary, for the weldment (Fig.2 c, d), initial softening was observed in all the test conditions. However, there are some difference between continuous low cycle fatigue and creep-fatigue. In the continuous test, the tensile peak stress keep decreasing through the fatigue life, it is hard to find the saturation stage, especially at high strain amplitude. Whereas in creep-fatigue, the tensile peak stress remains stable within a period before the final failure, even though some micro-crack might have already initiated. It indicates that there should be a mechanism to counteract the continuous softening at this period. For the low cycle fatigue tests performed, the total strain amplitude, $\Delta\varepsilon_t/2$, was chosen as controlling parameter. However, the parameter mainly determining the dislocation structure and thus the hardening/softening behavior is the plastic strain component, $\Delta\varepsilon_p/2$. $\Delta\varepsilon_p/2$ was found to change during the initial cycles

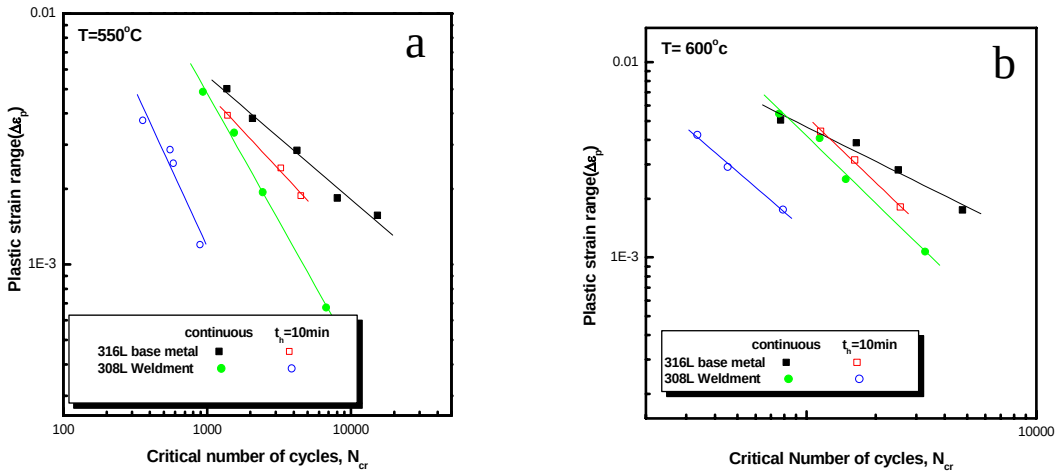

Fig. 3. Coffin-Manson plots for continuous low cycle fatigue and creep-fatigue at a) 550°C; b) 600°C

until a fairly constant value was reached and remained stable for most of the fatigue life. The immediate softening for the low amplitude results in a monotonic increase in $\Delta\varepsilon_p/2$. The initial hardening before softening for the highest strain amplitudes gives a slight decrease in $\Delta\varepsilon_p/2$ before it increases towards the stable value. If instead, the tests had been performed at constant $\Delta\varepsilon_p/2$ corresponding to those of the saturation regions in Fig.2 a, b, the initial hardening/softening behavior would have been more pronounced.

Plastic strain amplitude–life time relation.

The Coffin–Manson diagrams resulted from the specimens cycled to failure are presented in Fig. 3. It shows that the fatigue lives of weldment of both the continuous and creep-fatigue are shorter than those of base metal. In continuous case, the fatigue life of weldment is about 2/3 of that of base metal, whereas in creep-fatigue, the fatigue life of weldment is decreased to less than 1/3 of the life of base metal at the same strain amplitude. This means a more serious damage occurred in weldment during creep-fatigue. In addition, a lower slope was observed in base metal continuous test curve. It implies that even though the fatigue life of base metal at higher strain amplitude is almost same as weldment, it will be much longer at low strain amplitude.

3.3. Dislocation structures

The dislocation structures obtained from deformed specimens are given in Fig. 4 and 5. Cell structure was found in the base metal specimen subjected to continuous low cycle fatigue (Fig. 4a). However, the dislocation structure is different from grain to grain. It is to say that some grains have well developed cell structure, and some grains just have not fully developed wall structure. The same micro structure was observed in creep-fatigued base metal specimen, Fig. 4b shows the loose wall and cell structure at both sides of a twin boundary, respectively. This implies that the deformation within the specimen is not

uniform, the grains with easy to slip orientation might have subjected to higher local strain. In continuous tested weldment specimen, cell structure was also found in the austenite matrix, and it was separated by the δ-ferrite (Fig. 5a). However, in creep-fatigue tested weldment specimen, well developed subgrains were observed all around the observable area (Fig. 5b).

3.4. Precipitations

Fig. 6 and 7 shows the precipitations at δ-ferrite for different test conditions. Extremely fine carbides precipitated inside the δ-ferrite in base metal during both continuous and creep-fatigue test (Fig. 6a, b). Some bigger sized carbides were also found within the δ-ferrite in creep-fatigue tested specimens. The shape of δ-ferrite didn't change in base metal. Because of the low carbon content, there are not too many precipitations at the grain boundary and the austenite matrix after both continuous and creep-fatigue test. It was reported that the δ-ferrite in weldment is generally subjected to more rapid degradation than in base metal [11, 14]. In the present study, it was found that the morphδ-ferrite after continuous and creep-fatigue test is different in weldment. During continuous test, only some parts of the δ-ferrite were changed into carbide (arrow indicated in Fig. 7a). Whereas in creep-fatigue test, most of the δ-ferrite were changed into carbide, and it broken into short pieces after the test (Fig. 7b).

4. Discussions

4.1. Cyclic hardening/softening

The hardening behavior of 316L base metal during continuous low cycle fatigue and creep-fatigue is similar as previous workers [15, 16]. It could be explained by the increasing of dislocation density and the formation of dislocation substructures such as wall and cell structures. The continuous softening in 308L weldment during continuous low cycle fatigue could be attributed to the rearrangement of dislocations. Even though there are some cell structure formed, it didn't covered all the specimen. However, during creep-fatigue, subgrains were fully developed all over the specimen, this will retard the movement of gliding dislocations. Further more, as mentioned before, almost all of the δ-ferrite was changed into brittle carbide during creep-fatigue test, which will consequently make it more difficult for further deformation. That also might be one of the reasons for the broken of the carbide after creep-fatigue test.

4.2. Fatigue life and damage mechanism

It was widely reported that the shorter fatigue life-time during creep-fatigue with tensile hold is due to the nucleation of cavities at the grain boundary carbide [9, 10]. In the present study, because of the low carbon content in base metal, the number of grain boundary carbide was rather limited. So that its creep-fatigue resistance is higher than that of higher carbon content stainless steels, such as 316 SS and 304SS [17, 18]. There are many carbide precipitations inside the δ-ferrite, however, no carbides was found at the δ-ferrite/matrix interface. There is no evidence that cavity could nucleate around the carbide inside δ-ferrite, so we can expect that this kind of precipitation has no effect on the creep-fatigue resistance of 316L base metal. In case of weldment, the damage mechanism is rather complex. Firstly, the weldment, HAZ and base metal have different inelastic properties. During plastic deformation, the strain could be concentrated on some

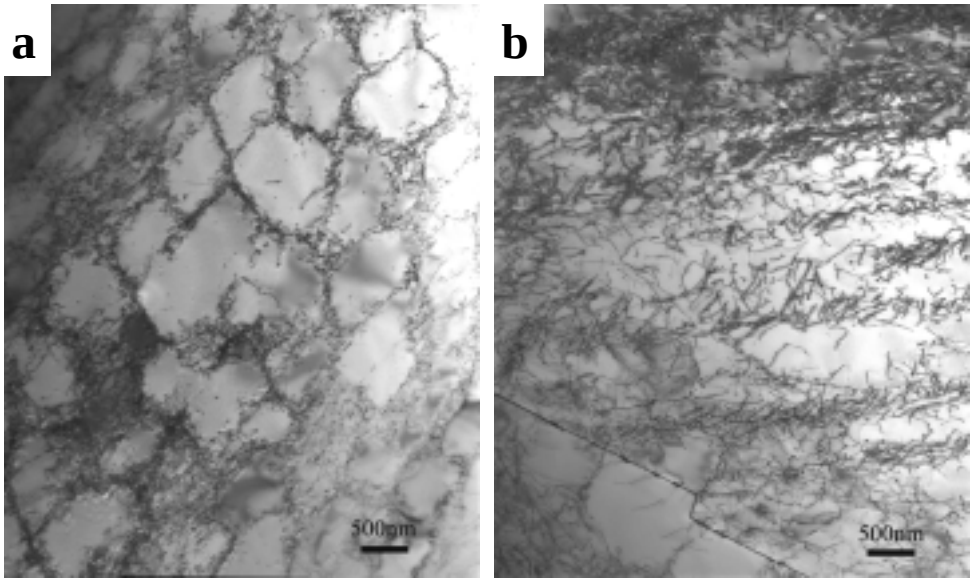

Fig. 4. Dislocation structure of 316L base metal: a) after LCF at 600^{o}C, $\Delta\varepsilon_t$=±0.5%; b) after creep-fatigue test at 600^{o}C, $\Delta\varepsilon_t$=±0.5%, t_h=10min.

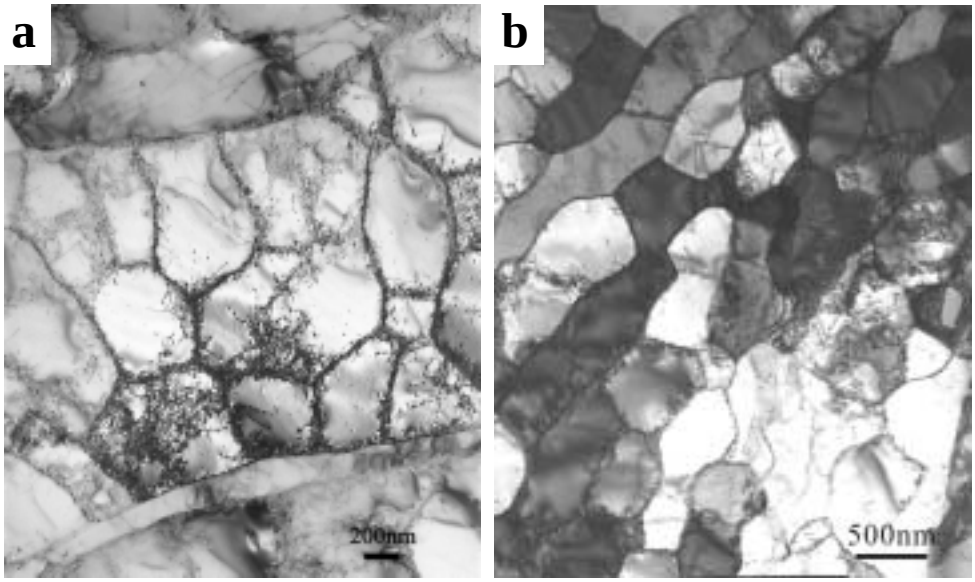

Fig. 5. Dislocation structure of 308L weldment: a) after LCF at 550^{o}C, $\Delta\varepsilon_t$=±0.5%; b) after creep-fatigue test at 600^{o}C, $\Delta\varepsilon_t$=±0.5%, t_h=10min.

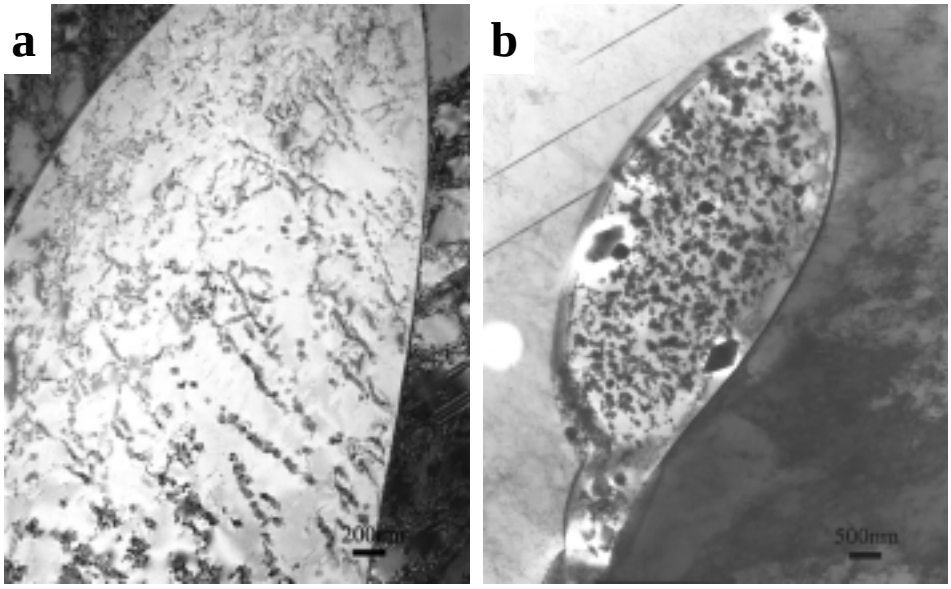

Fig. 6. δ-ferrite morphology of 316L base metal: a) after LCF at 550^{o}C, $\Delta\varepsilon_t$=±0.5%; b) after creep-fatigue test at 600^{o}C, $\Delta\varepsilon_t$=±0.5%, t_h=10min.

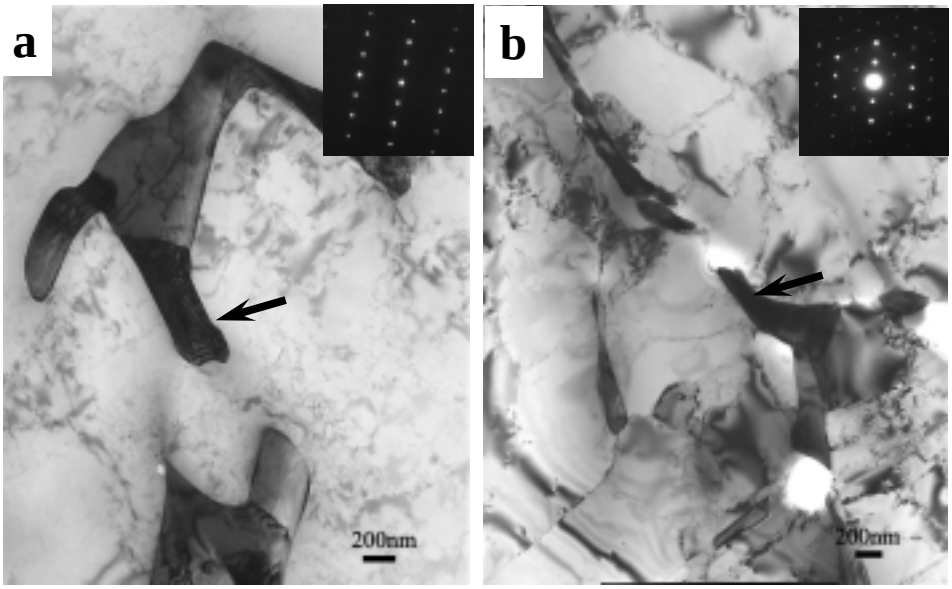

Fig. 7. δ-ferrite and carbide morphology of 308L weldment: a) after LCF at 600^{o}C, $\Delta\varepsilon_t$=±0.5%, b) after creep-fatigue test at 600^{o}C, $\Delta\varepsilon_t$=±0.5%, t_h=10min. (Arrow indicates carbides)

local areas within the welded joint, which will lead to a more rapid failure. Secondly, the strength varies within the welded joint, that is, creep-fatigue resistance of the weldment is generally weaker than that of the base metal. As the content of δ-ferrite is higher in the weldment than in the base metal, the weldment is subjected to more rapid degradation

than the base metal, which could lead to the reduction of long-term creep–fatigue life of welded joints [19]. This mechanism takes place regardless of the strain range. In the present work, the transformation from δ-ferrite to carbide is observed in both continuous and creep-fatigue tested specimens. After creep-fatigue, carbide occupied the area where the δ-ferrite had located before test, as shown in Fig. 8. The δ-ferrite/austenite interface was taken place by the carbide/austenite interface, where the cavity is more easily to nucleate. As a result, the crack propagation mode is different for continuous low cycle fatigue and creep-fatigue. During continuous low cycle fatigue (Fig. 9a), crack propagates regardless of the dendrite structure of δ-ferrite. Whereas in creep-fatigue, micro-crack initiates and propagates along the dendrite structure which is occupied by carbide (Fig. 9b). It implies that the weaker carbide/austenite interface caused the reduction of creep-fatigue life.

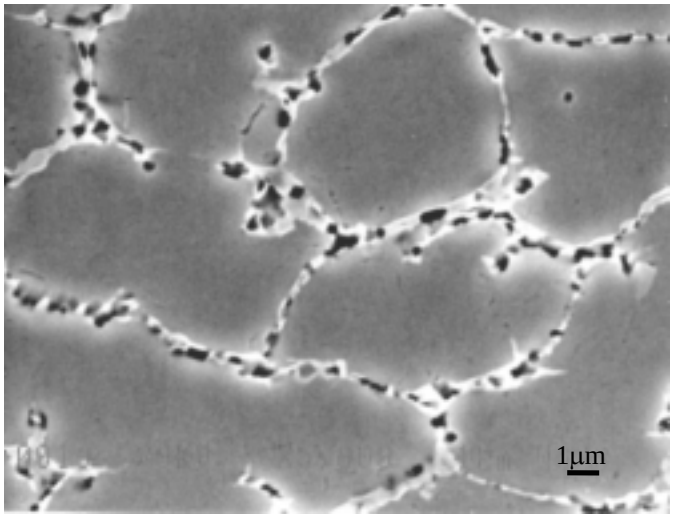

Fig. 8. Carbide morphology after creep-fatigue test at 550^{o}C, $\Delta\varepsilon_t$=±0.6%, t_h=10min.

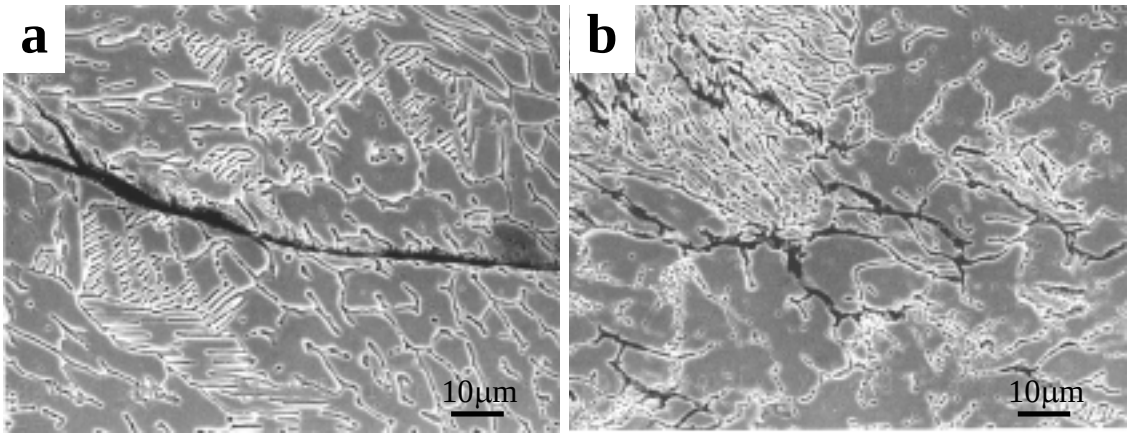

Fig. 9. SEM micrographs of crack in weldment, a) Continuous LCF; b) Creep-fatigue

5. Conclusions

The cyclic deformation characteristics and fatigue behavior of a 316L austenitic stainless steel and 308L weldment have been studied. Detailed studies were performed on the cyclic stress–strain behaviour, fatigue lifetime, dislocation structure as well as precipitations during test. According to the results, conclusions can be drawn as below:

1. Immediate cyclic hardening in 316L base metal during both continuous low cycle fatigue and creep-fatigue was observed. For 308L weldment, continuously softening through the fatigue life in continuous low cycle fatigue test occurs. Whereas in creep-fatigue, saturation stage before the final failure is observed.
2. The hardening of base metal is due to the increasing of dislocation density and the formation of dislocation substructures such as wall and cell structures. The softening of weldment is resulted from the rearrangement of dislocations. Fully developed subgrains and the transformation from δ-ferrite to carbide might be the reason for the occurrence of saturation stage in creep-fatigue in weldment.
3. Lower the carbon content may increase the creep-fatigue resistance of base metal.
4. The fatigue lives of weldment of both the continuous and creep-fatigue are much shorter than that of base metal. The weaker carbide/austenite interface formed during creep-fatigue test caused the reduction of creep-fatigue life for weldment.

REFERENCES

1. D.N. French, Metallurgical Failures in Fossil Fired Boilers, 2nd edn., Wiley, New York, (1993) p. 2.
2. E.G. Ellison, A.J.F. Paterson, Proc. Inst. Mech. Eng. 190 (1976) p.333
3. S. Heino, B. Karlsson, Acta mater. 94 (2001) p.339
4.. C.R. Brinkman, G.E. Korth, R.R. Hobbins, Nucl. Tech. 16 (1972) p.297
5. J. Wareing, Metall. Trans. A 8A (1978) p.711.
6. J.W. Hong, S.W. Nam, K.-T. Rie, J. Mater. Sci. 20 (1985) p.3763
7. S. W. Nam, Mater. Sci. Eng. A 322 (2002) p.64
8. P. Agatonovic, N. Taylor, Proc. 4th Int. Conf. on Creep and Fracture of Engineering Materials and Structures, April 1–6, (1990), p. 803.
9. B.G. Choi, S.W. Nam, Y.C. Yoon, J.J. Kim, J. Mater. Sci. 31 (1996) p.4957
10. R. Raj, M.F. Ashby, Acta Metal. 23 (1975) p.653
11. M.D. Mathew, G. Sasikala, te al, Mater. Sci. Tech. 7 (1991) p.533
12. C.C. Tsang, Y. Shen, et al, Metall. Trans. 25A (1994) p.1147
13. V.S. Srinivasan, R. Sandhya, et al, Int. J. Fatigue, 13 No.6 (1991) p471
14. Tai Asayama, Nuclear Engineering and Design 198 (2000) p.25
15. R. Alain, P. Violan, J. Mendez, MSE A 229 (1997) p.87
16. M. Gerland et al., MSE A118 (1989) p.83
17. J.M. Lee, S.W. Nam, Int. J. Damage Mechanics, 2 January (1993) p.4
18. S.W Nam, et al, Metall. Mater. Trans. A 27A, May (1996) p.1273
19. S.C. Tjong, S.M. Zhu, N.J. Ho, J.S. Ku, J. Nuclear Mater. 227 (1995) p.24